Materials Science and Engineering C 33 (2013) 4512–4519

Contents lists available at ScienceDirect

Materials Science and Engineering C

journal homepage: www.elsevier.com/locate/msec

Effects of surface modification on the mechanical and structural properties of nanofibrous poly(ε-caprolactone)/forsterite scaffold for tissue engineering applications

M. Kharaziha [a,b,*], M.H. Fathi [a,c], H. Edris [a,b]

[a] Biomaterials Research Group, Department of Materials Engineering, Isfahan University of Technology, Isfahan 8415683111, Iran
[b] Department of Materials Engineering, Isfahan University of Technology, Isfahan 8415683111, Iran
[c] Dental Materials Research Center, Isfahan University of Medical Sciences, Isfahan, Iran

ARTICLE INFO

Article history:
Received 2 April 2013
Received in revised form 5 June 2013
Accepted 4 July 2013
Available online 12 July 2013

Keywords:
Surface modification
Bone tissue engineering
Composite fibrous scaffolds
Electrospinning

ABSTRACT

Composite scaffolds consisting of polymers reinforced with ceramic nanoparticles are widely applied for hard tissue engineering. However, due to the incompatible polarity of ceramic nanoparticles with polymers, they tend to agglomerate in the polymer matrix which results in undesirable effects on the integral properties of composites. In this research, forsterite (Mg_2SiO_4) nanoparticles was surface esterified by dodecyl alcohol and nanofibrous poly(ε-caprolactone)(PCL)/modified forsterite scaffolds were developed through electrospinning technique. The aim of this research was to investigate the properties of surface modified forsterite nanopowder and PCL/modified forsterite scaffolds, before and after hydrolytic treatment, as well as the cellular attachment and proliferation. Results demonstrated that surface modification of nanoparticles significantly enhanced the tensile strength and toughness of scaffolds upon 1.5- and 4-folds compared to unmodified samples, respectively, due to improved compatibility between matrix and filler. Hydrolytic treatment of scaffolds also modified the bioactivity and cellular attachment and proliferation due to greatly enhanced hydrophilicity of the forsterite nanoparticles after this process compared to surface modified samples. Results suggested that surface modification of forsterite nanopowder and hydrolytic treatment of the developed scaffolds were effective approaches to address the issues in the formation of composite fibers and resulted in development of bioactive composite scaffolds with ideal mechanical and structural properties for bone tissue engineering applications.

1. Introduction

Nanophase forsterite (Mg_2SiO_4) has recently been introduced as a bioceramic [1,2]. It posses excellent in vitro apatite formation ability and bioactivity [2], improved mechanical properties compared to the other bioactive ceramics such as Hydroxyapatite(HA) and approved cellular interactions which make it a good candidate for bone tissue engineering application [3]. According to the natural bone structure consisting of HA embedded in a collagen matrix, a combination of a synthetic or natural polymer and a bioactive ceramic could increase the mechanical properties and hydrophilicity, induce osteoconductivity and/or osteoinductivity and improve cellular affinities [4,5].

Diba et al. [6] fabricated poly(ε-caprolactone)(PCL)/forsterite porous scaffolds through solvent-casting/particle-leaching technique and confirmed the bioactivity of composite structures [6,7]. In order to simulate the fibrous structure of bone extracellular matrix (ECM) which is the vital factor to promote cellular behavior [8], we recently developed nanofibrous composite scaffolds of PCL/forsterite [9]. Results demonstrated that forsterite nanopowder significantly improved the attachment, proliferation and mineralization of MC3T3-E1 cells compared to pure PCL fibrous scaffolds [9]. However, at high forsterite content scaffolds (20 wt.%), due to the small dimensions and incompatible polarity of forsterite nanopowder with polymer matrix, the particles intended to agglomerate in the polymer matrix which resulted in attenuation the integral property of the composite, specifically mechanical characteristics [7,9].

The surface modification of nanoparticles using organic molecular is a promising approach in order to provide the effective interfacial adhesion and uniform dispersion of nanoparticle in the polymer matrix [10–17]. Esterification reaction using dodecyl alcohol is an effective method for surface modification of silicates [18], bioglass (BG) [19] and hydroxyapatite (HA) [11]. It consists of a reaction of alcohol groups of dodecyl alcohol with acidic functional groups on the surface of nanophase ceramics to form an ester. However, reduced hydrophilicity is the disadvantage of the modification with dodecyl alcohol, which affected the protein adsorption and consequent cellular attachment and proliferation on the structures [20]. So, it would be great if the dodecyl chains were removed

* Corresponding author at: Biomaterials Research Group, Department of Materials Engineering, Isfahan University of Technology, Isfahan 8415683111, Iran. Tel.: +98 3912750; fax: +98 3912752.
E-mail address: Kharaziha.ma@yahoo.com (M. Kharaziha).

0928-4931/$ – see front matter © 2013 Elsevier B.V. All rights reserved.
http://dx.doi.org/10.1016/j.msec.2013.07.002

from surface of nanophase ceramics after uniform distribution in polymer matrix.

The surface modification based on esterification reaction is reversible through hydrolysis under certain conditions. Results demonstrated that the dodecyl alcohol linked on the surface of nanoparticles such as $CaSiO_3$ particles could be removed through the hydrolytic treatment [20]. The focus of this research is to surface modify forsterite nanoparticle using dodecyl alcohol and characterize esterified forsterite nanoparticle and the nanofibrous composites of PCL/modified forsterite. Furthermore, the removal of dodecyl alcohol chains after surface modification and the properties of the composite materials after hydrolytic treatment were also investigated.

2. Materials and methods

2.1. Surface modification and hydrolytic treatment of forsterite nanopowder

Forsterite nanopowder was prepared by using sol–gel method as described in our previous research [2]. Surface esterification of forsterite nanopowder by dodecyl alcohol was conducted according to the procedure reported recently for the other nanophase ceramics [18]. In brief, a suspension of forsterite nanopowder in 95% (v/v) ethyl alcohol was dispersed by 15 min ultrasonic treatment technique. After evaporation of ethyl alcohol, forsterite nanopowder was ultrasonically dispersed in dodecyl alcohol for 15 min and followed by 4 h stirring. The esterification reaction was completed at 260 °C for 4 h and surface modified forsterite nanopowder (named as M-Mg_2SiO_4) was obtained through centrifugation, washing with ethyl alcohol and finally drying at 60 °C. The modification process is schematically presented at Fig. 1.

The hydrolytic treatment of forsterite nanopowder was conducted under immersing at two mediums; deionized water (at room temperature) for 24 h (named as MH(C)-Mg_2SiO_4) and boiled water for 30 min (named as MH(H)-Mg_2SiO_4) and followed by filtering and drying at room temperature.

2.2. Development of nanofibrous PCL/modified forsterite scaffolds

Nanofibrous composite scaffolds consisting of modified forsterite nanopowder were developed through electrospinning technique similar to our previous report [9]. Poly(ε-caprolactone)(PCL)(M_w = 80,000 g/mol) solution was prepared at the concentration of 10% (w/v) in (9:1) chloroform:ethanol solution. After dissolving PCL, modified forsterite nanopowder at concentrations of 5 and 20 wt.% was added and constant amount of 0.06% w/v NaCl was applied in order to increase conductivity of the solutions. Unmodified forsterite nanopowder (named as U-Mg_2SiO_4) was also applied as a control. The prepared solutions were sonicated for 1 h and fed into a 1 mL standard syringe equipped with a 23 G blunted stainless steel needle using a syringe pump. The flow rate (2 mL/h), the distance between the needle and the collector (18 cm) and the electrospun voltage (20 kV) were optimized and kept constant during the electrospinning process. Composite nanofibrous scaffolds consisting of various kinds of forsterite nanopowders (unmodified (U-Mg_2SiO_4) and modified (M-Mg_2SiO_4)) were spun and deposited on the glass slides placed on the collector plate. The scaffolds were named as PCL-5(U-Mg_2SiO_4), PCL-5(M-Mg_2SiO_4), PCL-20(U-Mg_2SiO_4) and PCL-20(M-Mg_2SiO_4), respectively, where letters U and M define the type of forsterite nanopowder (unmodified and surface modified, respectively) and 5 and 20 correspond to 5 wt.% and 20 wt.% forsterite nanopowder content, respectively. The developed scaffolds were dried overnight under vacuum condition prior to further characterizations and biological experiments.

Nanofibrous PCL/M-Mg_2SiO_4 scaffolds were also hydrolytic treated under the same process as described for M-Mg_2SiO_4 nanopowders in deionized water (at room temperature) (named as PCL/5 wt.%(MH(C)-Mg_2SiO_4) or PCL-5(MH(C)-Mg_2SiO_4), PCL/20 wt.%(MH(C)-Mg_2SiO_4) or PCL-20(MH(C)-MH(C)-Mg_2SiO_4)) and boiled water (named as PCL/5 wt.%(MH(H)-Mg_2SiO_4) or PCL-5(MH(H)-Mg_2SiO_4) and PCL/20 wt.%(MH(H)-Mg_2SiO_4) or PCL-20(MH(H)-Mg_2SiO_4)), respectively.

2.3. Characterization of surface modified and hydrolytic treated forsterite nanopowders and nanofibrous PCL/forsterite scaffolds

The chemical characteristics of unmodified, surface modified and hydrolytic treated forsterite nanopowders were investigated by using Fourier-transform infrared (FTIR) spectroscopy (Bomem, MB 100). Dispersion stability of nanopowders (unmodified, surface modified and hydrolytic treated nanopowder) was determined by sedimentation experiments in two various mediums; water and chloroform according to the previous report [19]. In a brief, the nanopowders at a solid loading of 1 g/L ultrasonically dispersed in above mediums. The sedimentation behavior was estimated according to the required time in which all of nanoparticles receipted out of the solution and the medium became completely transparent.

The thermal properties of pure PCL and nanofibrous PCL/forsterite scaffolds were determined by the differential scanning calorimetry (DSC) and thermogravimetric analysis (TGA) (Rheometric scientific 1998, USA) at a heating rate of 10 °C/min in flowing nitrogen gas in order to investigate the effects of surface modification of forsterite nanopowder on the melting temperature, melting enthalpy and crystallinity, X_c, of PCL matrix. Crystallinity of PCL was calculated according to the following Eq. (1):

$$X_c = \frac{\Delta H_m}{\Delta H_{m,100\%}} \quad (1)$$

where ΔH_m indicated the melting enthalpy for the scaffold, and $\Delta H_{m,100\%}$ was the theoretical enthalpy of completely crystalline PCL which was about 142 J/g [21].

Nanofibrous scaffolds were gold-sputter-coated and their surface topographies were characterized using scanning electron microscopy (SEM; Philips XL30, USA) and average fiber sizes (n = 50) of the scaffolds were then analyzed using the SEM images and (NIH) Image J software. Furthermore, forsterite nanopowder distribution in the nanofibers was evaluated by transmission electron microscopy (TEM; EML, Zeiss, Germany).

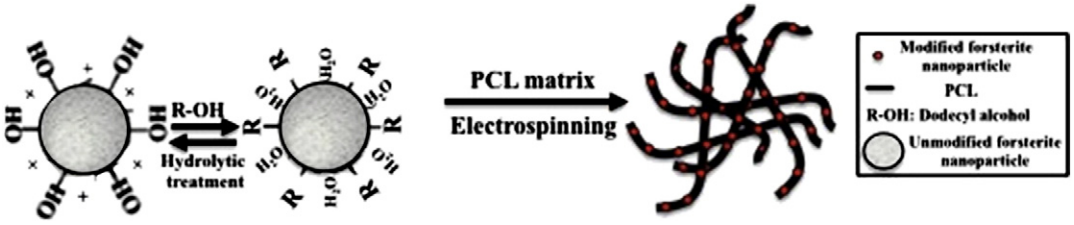

Fig. 1. Schematic of the surface modification process of forsterite nanopowder and nanofibrous PCL/forsterite scaffold formation.

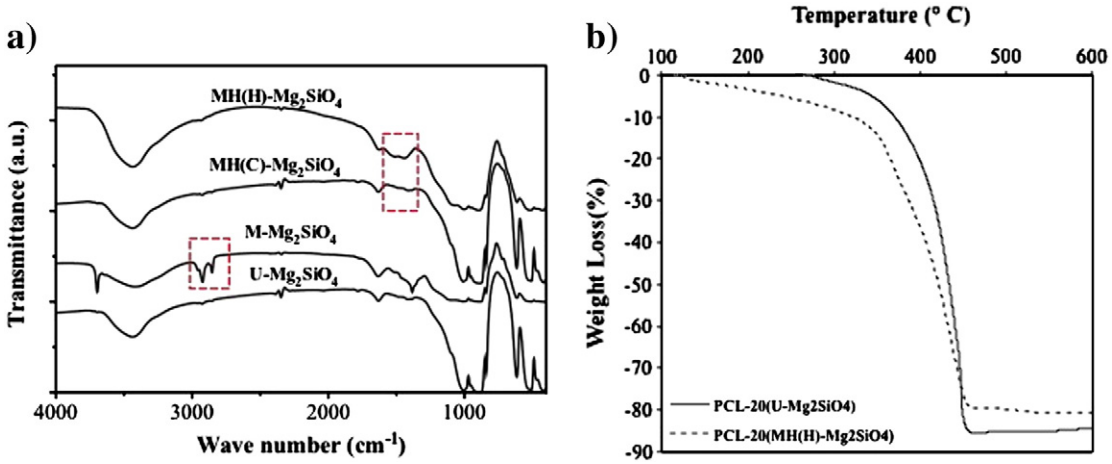

Fig. 2. Structural properties of forsterite nanopowder and fibrous scaffolds: (a) FTIR spectra of unmodified (U), surface modified (M), Hydrolytic treated at boiled water (MH(H)) and cold water (MH(C)) forsterite nanopowder. (b) TGA of PCL-20(U-Mg_2SiO_4) and PCL-20MH(H)-Mg_2SiO_4) fibrous scaffolds.

The tensile properties of the nanofibrous scaffolds were determined using uniaxial testing instrument (INSTRON, Zwick, United Kingdom) with 10 N load capacity and a cross-head speed of 7 mm/min. The samples were prepared in a rectangular shape with dimensions of 10×50 mm^2 and precise thicknesses assessed using a micrometer. At least 5 samples were prepared for each type of the nanofibrous scaffolds. Ultimate strength (maximum stress that sample could achieve), tensile modulus (slope of the initial linear part of the stress–strain curve), energy per volume (the area under the stress–strain curve) and strain at break (maximum strain before the failure) of the samples were determined from the tensile stress–strain curves. The results were reported as average value and standard deviations.

2.4. Degradation study of the nanofibrous scaffolds

In vitro degradation assay was used to study the weight loss of the nanofibrous scaffolds within 4 weeks soaking in Phosphate buffered saline (PBS) (Sigma). PBS was changed every 3 days and after each specific time point, pH of PBS was determined by using pH meter (Metrohm, Germany). The scaffolds were rinsed in PBS, freeze-dried overnight and the degradation percentage of each sample was calculated by dividing the weight loss to the first dry weight. The results were expressed as average value and standard deviations.

2.5. Bioactivity study of the nanofibrous scaffolds

The bioactivity was assessed through the soaking of the scaffolds in simulated body fluid (SBF) prepared according to Kokubo protocol [22]. The samples ($n = 3$) with dimensions of 5×5 cm^2 were put in the polyethylene containers and maintained at 37 °C upon a month. The formation of apatite layer on the scaffolds was verified by SEM and determination of the concentration of Ca, Mg and P ions using inductively coupled plasma atomic emission spectroscopy (ICP) (AES; Varian, USA).

Table 1
Effect of surface modification and hydrolytic treatment on the dispersion stability of forsterite nanopowder.

Complete sedimentation time	U-Mg_2SiO_4	M-Mg_2SiO_4	MH(H)-Mg_2SiO_4	MH(C)-Mg_2SiO_4
Water	3 h	–	1 h	10 mm
Chloroform	10 min	5 h	15 min	3 h

"–": The sedimentation time is too short which could not be recorded.

2.6. In-vitro cellular assays

In order to evaluate the effects of surface modification of forsterite nanopowder and hydrolytic treatment of the nanofibrous scaffolds, MC3T3-E1 pre-osteoblast (sub-clone 14) cells were cultured on the scaffolds and cell attachment and proliferation were studied. The pre-osteoblast cells were cultured in Alpha Minimum Essential Medium (α-MEM, Cellgro, Mediatech, Manassas, VA, USA) supplemented with 10% fetal bovine serum (FBS, Cellgro, Mediatech, Manassas, VA, USA) and 1% streptomycin/penicillin (Cellgro, Mediatech, Manassas, VA, USA). Before cell seeding, the nanofibrous scaffolds were sterilized under 30 min soaking in 70% ethanol, overnight UV light and finally immersed in culture medium overnight before cell seeding. Cells (within passages 18–20) at a density of 3×10^4 mL^{-1} were seeded onto the scaffolds and tissue culture polystyrene (TCP) applied as a control.

The cell attachment on the nanofibrous scaffolds was determined using DNA quantification assay (Quant-iT™ PicoGreen®, Invitrogen, USA), according to the manufacturer's protocol. Membranes ($n = 3$) were rinsed with Dulbecco's phosphate buffered saline (DPBS, Gibco, USA) and weighed at wet condition. The samples were then digested overnight at 60 °C in 1 mL of DNA extraction solution. In order to prepare DNA extracted solution, PBE buffer was prepared by dissolving Na_2HPO_4 and EDTA (Sigma-Aldrich) in deionized water and adjusting the pH to 6.5 using 1 M HCl solution. Following, L-cystein was added to 20 mL of DNA extracted solution and the prepared solution was mixed with papain (0.5% (v/v)). Finally, 1× PicoGreen solution (50% (v/v)) was added to digested sample solution (50% (v/v)) and their absorbance was measured at 485 nm wavelength.

The pre-osteoblast metabolic activity on the scaffolds was determined by using the Alamar blue (AB) assay according to the manufacturer's protocol (Invitrogen) at days 0 (6 h), 3 and 7 of culture. Briefly, AB solution dissolved in warm culture medium was added into each well and incubated for 3 h. Then, reduced-color

Table 2
Effect of surface modification and hydrolytic treatment on the thermal properties of nanofibrous PCL/forsterite scaffolds determined by DSC and TG analyses.

Sample	T_m (°C)	ΔH_m (J/g)	X_c (%)	Weight loss (%)
PCL	57	54.5	38.4	98.6
PCL-5(U-Mg_2SiO_4)	56.5	51.6	36.3	96.1
PCL-5(MH(H)-Mg_2SiO_4)	59.2	56.7	39.8	94.5
PCL-20(U-Mg_2SiO_4)	55.8	43.8	30.6	83.5
PCL-20(MH(H)-Mg_2SiO_4)	62.1	59.1	41.6	79.3

T_m: Melting temperature, ΔH_m: melting enthalpy, X_c: crystallinity degree.

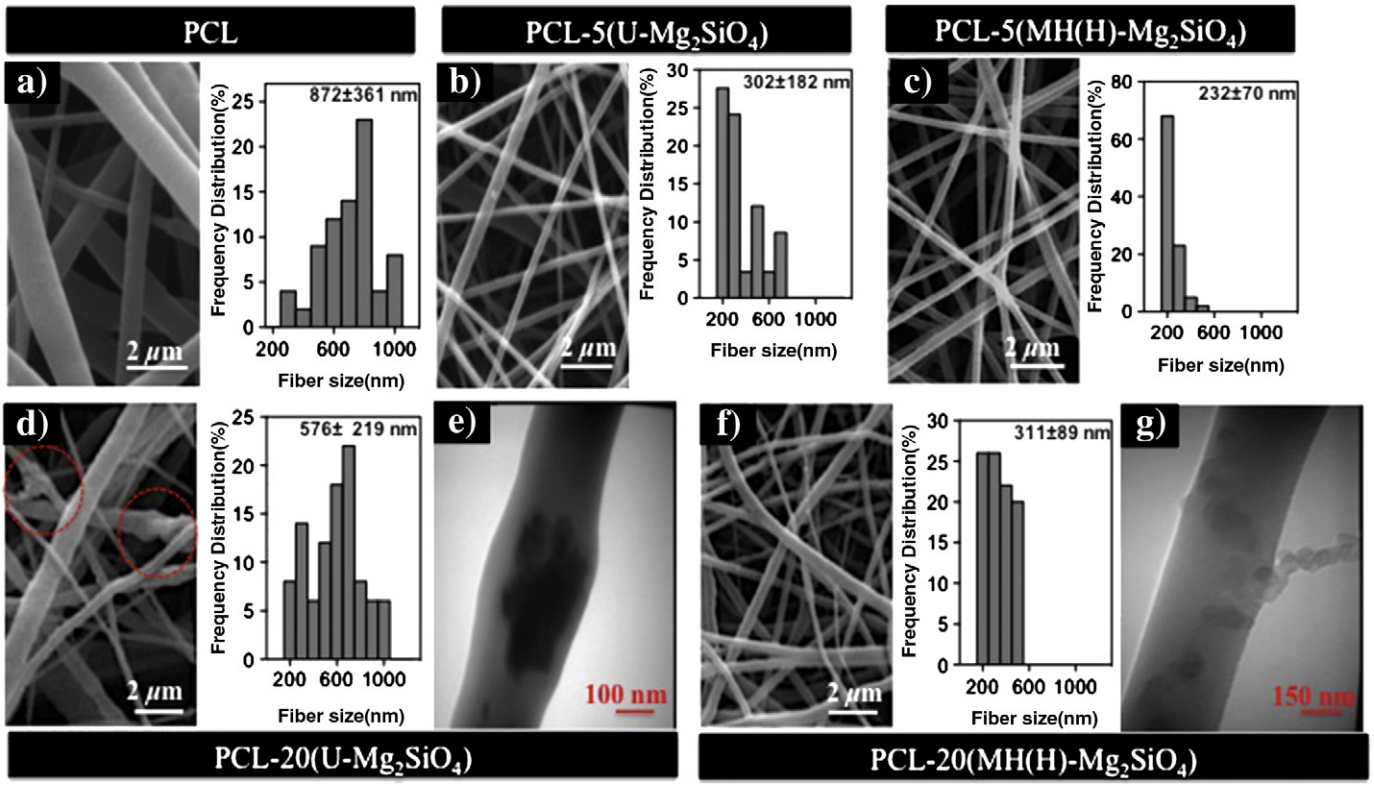

Fig. 3. Structural properties of the scaffolds and forsterite nanopowder: SEM images and the corresponding fiber size distribution of (a) pure PCL, (b) PCL/5 wt.%(U-Mg_2SiO_4), (c) PCL/5 wt.%(MH(H)-Mg_2SiO_4), (d) PCL/20 wt.%(U-Mg_2SiO_4) and (f) PCL/20 wt.%(MH(H)-Mg_2SiO_4) fibrous scaffolds. TEM micrographs of (e) PCL/20 wt.%(U-Mg_2SiO_4) and (g) PCL/20 wt.%(MH(H)-Mg_2SiO_4) scaffolds.

culture medium within each well was transferred to 96-well plate in duplicate and absorbance was measured at 544–590 nm wavelength. Finally, the normalized metabolic activity with respect to day 0 was calculated for each scaffold.

The morphology of cells cultured on PCL/20 wt.%(MH(H)-Mg_2SiO_4) scaffold was also studied by SEM. After 7 days of culture, cells were fixed in 2.5% glutaraldehyde for 3 h at room temperature, dehydrated in a graded series of ethanol solution (50%, 70%, 80%, 90% and absolute ethanol) and finally air-dried. In order to study cell morphology, cell cultured samples were gold coated and studied by SEM (Philips XL30, USA).

2.7. Statistical analysis

Data were presented in mean ± standard deviation (SD). Statistical significance was measured by performing one-way ANOVA analysis and comparisons were made by Tukey's post-hoc test using GraphPad Prism Software (V.5). A P-value <0.05 was taken to be significant.

3. Results and discussion

3.1. Characterization of surface modified forsterite nanopowder and nanofibrous PCL/modified forsterite scaffolds

In order to improve the dispersion of forsterite nanopowder and enhance the compatibility between PCL matrix and the nanophase filler, forsterite nanopowder was surface modified using dodecyl alcohol. FTIR analysis as a powerful method to identify the functional groups was applied before and after surface modification and hydrolytic treatment of forsterite nanopowder suggesting dodecyl alcohol could be tightly absorbed on the surface of nanopowder by chemisorption (Fig. 2(a)). Compared to the characteristic peaks of U-Mg_2SiO_4, the additional absorption bands presented at 2963, 2927 and 2859 cm^{-1} in the spectrum of M-Mg_2SiO_4 were attributed to the C – H stretching vibrations. According to previous reports, these peaks were the result of surface-modified dodecyl chains [23,24]. Similar to studies on the other silicates (i.e. $CaSiO_3$) and according to Lewis acid–base theory, dodecyl alcohol accepted electrons from the surfaces of nanophase ceramics which resulted in the formation of acidic sites on them [18]. Then, under the optimized condition of esterification, the hydroxyl groups of dodecyl alcohol reacted with acidic sites of particle surfaces providing the esterified nanoparticles according to Eq. (2) (Fig. 1):

$$(Mg_2SiO_4)-H^+ + (\text{Dodecyl chains})-OH^- \rightarrow (Mg_2SiO_4)-(\text{Dodecyl chains}) + H_2O. \quad (2)$$

However, a recent study demonstrated that surface modification through dodecyl alcohol reduced the protein adsorption, cell attachment and proliferation ability on the surface of biomaterials due to decreased hydrophilicity [25]. So, after achievement of homogenous dispersion of nanophase ceramic in polymer matrix, hydrolytic treatment might be useful. The FTIR spectra verified that hydrolytic treatment removed the dodecyl alcohol linked on the surface of M-Mg_2SiO_4 nanoparticles (Fig. 2(a)). After hydrolytic treatment in boiled water and cold water (MH(H)-Mg_2SiO_4 and MH(C)-Mg_2SiO_4, respectively), the dodecyl chain bands significantly decreased and even they could not be distinguished in the samples treated in boiled water confirming that most long alkyl chains were removed. It was suggested due to more energy provided by boiled water, it was more efficient. On the other hand, the presence of a new band centered at 1500 cm^{-1} related to Si – OH confirmed the formation of this group on the surface of forsterite nanopowder. According to previous research, formation of this group enhanced hydrophilicity of scaffolds which resulted in enhanced interactions of scaffolds with biological fluid [20].

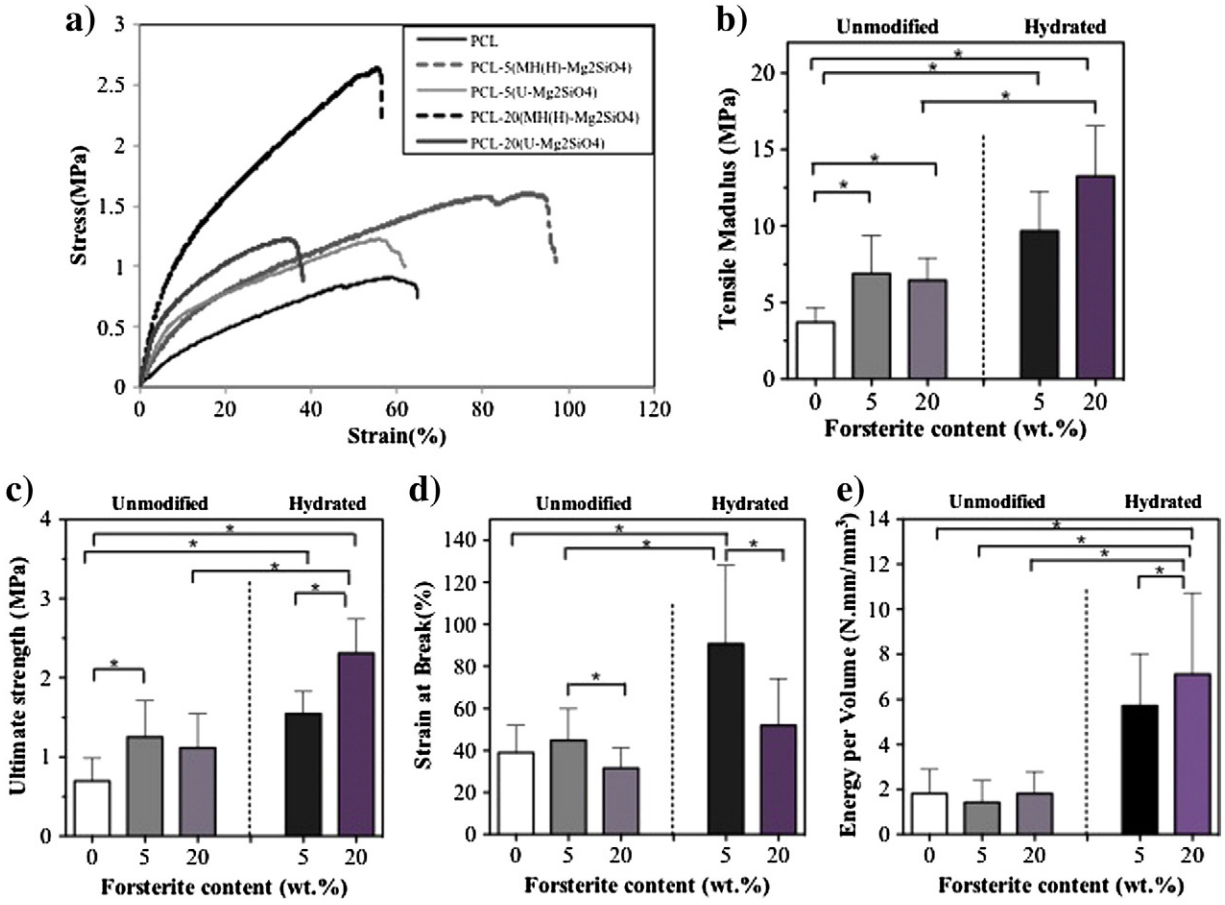

Fig. 4. Effects of surface modification and hydrolytic treatment processes on the mechanical properties of the scaffolds: (a) Representative tensile stress–strain curves, (b) tensile modulus, (c) ultimate strength, (d) strain at break and (e) energy per volume of nanofibrous PCL and PCL/forsterite scaffolds, before surface modification of forsterite nanopowder and after hydrolytic treatment of the scaffolds. (*: $P < 0.05$).

Interestingly, the dispersion stability results also changed after surface modification and hydrolytic treatment of particles which proved FTIR results (Table 1). While U-Mg_2SiO_4 nanoparticles were the most stable powder in water, the sedimentation of M-Mg_2SiO_4 was too fast which could not be recorded. After hydrolytic treatment, the sedimentation time of powders dramatically changed compared to M-Mg_2SiO_4 nanoparticles. In water (polar solvent), sedimentation time was much longer, while shorter than that of U-Mg_2SiO_4 suggesting hydrophobic alkyl chains on the surface of modified forsterite particles were reduced. Compared to polar solvent, in weakly polar solvent (chloroform), the sedimentation time of U-Mg_2SiO_4 nanoparticles decreased while three other types of forsterite nanopowders were more stable. Furthermore, the precipitation of MH(H)-Mg_2SiO_4 was the fastest.

The homogenous dispersion of forsterite nanopowder through PCL matrix also affected the thermal properties of fibrous scaffolds and true loading of forsterite nanopowder. After completely burning out of PCL content through TGA analysis, the true contents of forsterite nanopowder in the scaffolds were determined (Fig. 2(b) and Table 2). Results confirmed that surface modification increased the true forsterite content to reach the amount which was added to the starting solutions. It confirmed the good dispersion of forsterite nanopowder through PCL matrix (Table 2). According to data obtained from DSC curves, after surface modification, the melting temperature of scaffolds enhanced with increasing forsterite content which could be due to the interaction between PCL and forsterite nanopowder. Additionally, while the melting enthalpy of the scaffolds significantly reduced with increasing forsterite content, it slightly enhanced after surface modification of forsterite nanopowder. It was suggested the restricted mobility of PCL macromolecules due to improved interaction between two phases. Furthermore, the crystallinity did not significantly change at various scaffolds.

SEM images and the corresponded fiber size distributions and TEM micrographs of scaffolds consisting of various kinds of forsterite contents are presented in Fig. 3. According to SEM micrographs, the morphology and fiber size distributions of the nanofibrous scaffolds were the functions of forsterite content and treatment process. As reported before [9], while the incorporation of forsterite nanopowder upon 5 wt.% (Fig. 3(b)) reduced the average fiber sizes compared to pure PCL scaffold (Fig. 3(a)), higher forsterite content resulted in larger fiber size with extended distribution (Fig. 3(d)) [9]. According to TEM micrograph of PCL/20 wt.%(U-Mg_2SiO_4) (Fig. 3(e)), aggregated particles with a diameter of 500 to 1500 nm could be observed in this scaffold. As such agglomerates could not be found in the nanofibrous composite scaffolds loaded with surface modified forsterite nanopowder, even after hydrolytic treatment (Fig. 3(g)). According to TEM micrograph of PCL/20 wt.%(MH(H)-Mg_2SiO_4) (Fig. 3(g)), surface modification greatly improved the dispersion of forsterite nanopowder within PCL matrix. While surface modification of forsterite nanopowder did not significantly change the fiber size of PCL/5 wt.%(MH(H)-Mg_2SiO_4) (Fig. 3(c)) compared to unmodified sample (Fig. 3(b)), PCL/20 wt.%(MH(H)-Mg_2SiO_4) fibers (Fig. 3(f)) were significantly thinner with limited distribution than those in PCL/20 wt.%(U-Mg_2SiO_4) scaffold (Fig. 3(d)). Similar to typical bioceramics, forsterite nanopowder exhibited hydrophilicity, while PCL matrix is hydrophobic. In order to provide a stable suspension, the incompatible properties of two phases resulted in the agglomeration of

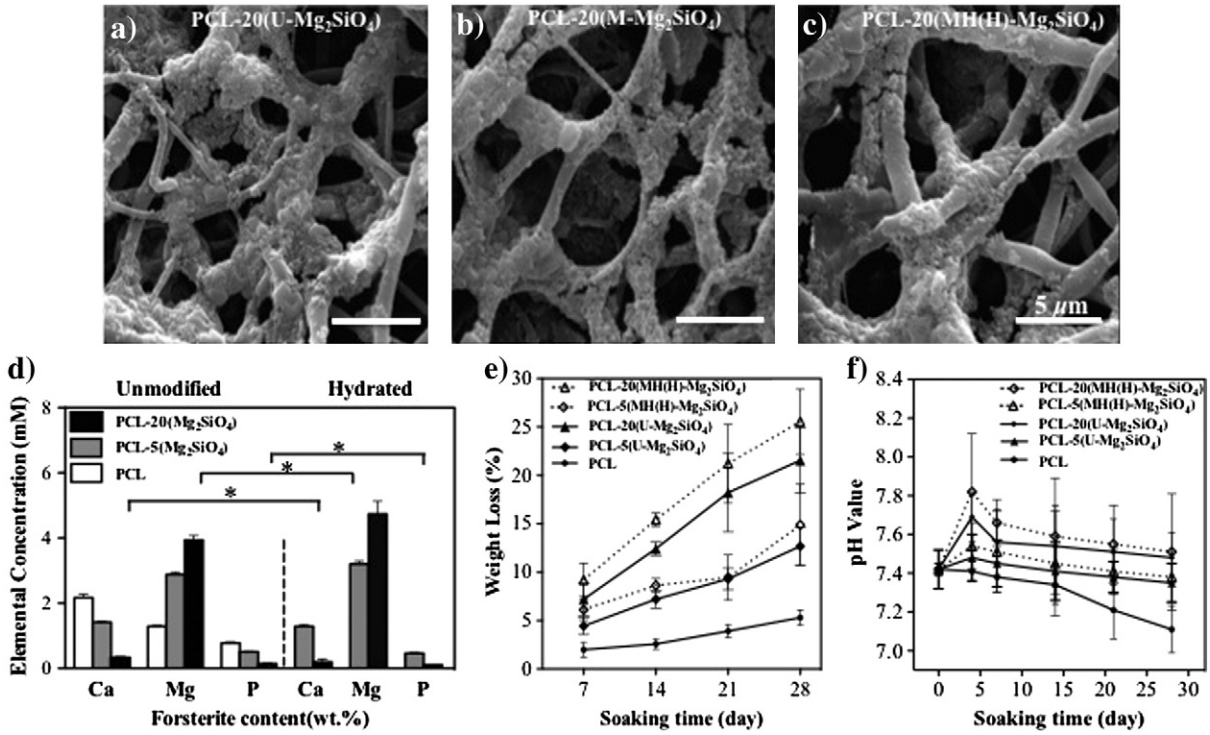

Fig. 5. Effects of surface modification and hydrolytic treatment processes on the bioactivity and degradation of PCL/forsterite scaffolds: SEM micrographs of (a) PCL-20(U-Mg_2SiO_4), (b) PCL-20(M-Mg_2SiO_4) and (c) PCL-20(MH(H)-Mg_2SiO_4) scaffolds and (d) Ca, Mg and P ion concentrations of SBF solution after 4 weeks immersion of the scaffolds (Scale bar = 5 μm). (*: $P < 0.05$). (e) Weight loss of fibrous scaffolds as function of soaking time in PBS and (f) pH trends of PBS during the immersing the scaffolds.

forsterite particles to each other following by the inhomogeneous dispersion of U-Mg_2SiO_4 in PCL matrix, increasing fibers sizes and broader fiber size distribution. After surface modification, due to repulsive forces from the interpenetration of dodecyl chains on the surface of forsterite particles, they organized in a nearly uniform dispersion in the suspension and fibrous structure.

The homogenous dispersion of forsterite nanoparticles into PCL matrix and their interactivity had significant effects on the properties of composites such as mechanical properties. The representative tensile stress–strain curves of PCL and composite scaffolds (Fig. 4(a)) exhibited similar trends. As strain continuously increased, the curves deviated from the linear proportionality and depending on forsterite content and its distribution in PCL matrix, they exhibited significant changes on the mechanical properties (Fig. 4(b–e)). Addition of forsterite nanopowder significantly improved the mechanical properties of the scaffolds ($P < 0.05$). However, before surface modification, due to agglomeration of particles and stress concentration occurred on the agglomeration place, the addition of unmodified forsterite nanopowder upon 20 wt.% resulted in decreased mechanical properties compared to PCL/5 wt.%(U-Mg_2SiO_4). After surface modification, mechanical properties significantly enhanced compared to PCL/unmodified forsterite scaffolds due to the better interactions between PCL and the dodecyl chains bonded to forsterite nanopowder and reduced stress concentration during uniaxial tensile test. In a recent report, surface modified HAp improved the mechanical strength of PCL/HAp scaffolds due to the enhanced adhesion at the organic–inorganic interface as well as the uniform

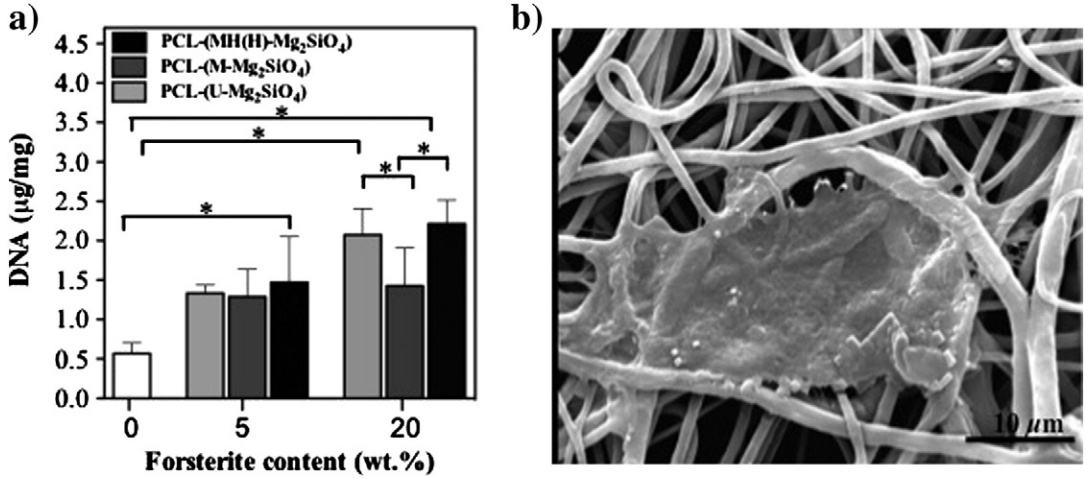

Fig. 6. Effects of surface modification and hydrolytic treatment processes on (a) the cellular attachment (PicoGreen assay) and (b) cell morphology after 7 days of culture on PCL/20 wt.%(MH(H)-Mg_2SiO_4) fibrous scaffold. (*: $P < 0.05$).

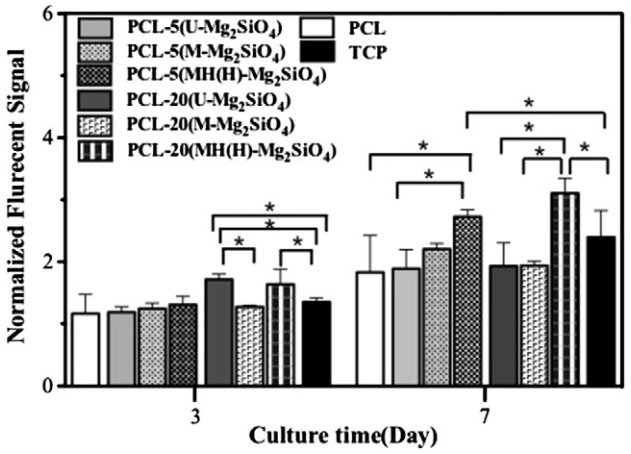

Fig. 7. Effects of surface modification and hydrolytic treatment processes on the proliferation (Alamar Blue assay) of MC3T3-E1 cells cultured on the nanofibrous scaffolds. (*: $P < 0.05$).

dispersion of HAp at nano-level [26]. In another experiment, BGs particles were surface modified by esterification reaction with dodecyl alcohol and poly-(D,L-lactic acid) (PDLLA)/modified BGs composite films showed more uniform particle distribution and enhanced mechanical strength compared to unmodified samples [27].

Besides mechanical properties, osteo-conductivity is another important characteristic of scaffolds for bone tissue engineering application. This property was evaluated by studying the ability of apatite formation on the scaffolds through incubation in SBF with ion concentrations equal to human blood plasma. SEM micrographs of PCL/20 wt.%(Mg_2SiO_4) scaffolds consisting of various kinds of forsterite nanopowder (unmodified, surface modified and surface modified nanoparticles followed by hydrolytic treatment of the scaffold) after 4 weeks incubation in the SBF (Fig. 5(a–c)) showed that bone like apatite was precipitated with similar morphology on the nanofibrous composite scaffolds. It suggested that the scaffolds were still bioactive after surface modification and hydrolytic treatment. In order to explain the effects of surface modification and hydrolytic treatment on the bioactivity mechanism, the cumulative variation of ion concentrations consisting of magnesium ions released from composites into SBF and calcium and phosphorus ions deposited from SBF on the scaffolds were estimated. According to Fig. 5(d), after surface modification, dissolved magnesium ions decreased while less calcium and phosphorus ions precipitated which might be due to enhanced hydrophobic property of forsterite nanoparticles. As bioactivity is the result of ion interactions between SBF and the scaffolds, it would be ideal to remove the dodecyl chains from composite nanofibrous scaffolds after achievement of uniform distribution of inorganic particles in polymer matrix. After hydrolytic treatment, released magnesium ions increased while calcium and phosphorus ions of SBF were significantly decreased compared to the surface modified and unmodified samples. It could be due to the presence of silanol groups on the surface of forsterite particles which enhanced nucleation sites for the deposition of calcium and phosphorus ions and the formation of bone-like apatite on the surface of fibrous scaffolds.

In vitro degradation of the scaffolds was monitored over a month period (Fig. 5(e)). The degradation rate of scaffolds could be modulated by addition of forsterite nanopowder as well as modification process. After a month of incubation, the weight loss of PCL scaffold was significantly ($P < 0.05$) less than others due to hydrophobicity property. At the end of the incubation, the weight losses of scaffolds were about $5.3 \pm 0.8\%$, $12.7 \pm 1.2\%$, $14.9 \pm 4.2\%$, $21.5 \pm 3.6\%$ and $25.6 \pm 3.4\%$ within PCL, PCL/5 wt.%(U-Mg_2SiO_4), PCL/5 wt.% (MH(H)-Mg_2SiO_4), PCL/20 wt.%(U-Mg_2SiO_4) and PCL/20 wt.%(MH (H)-Mg_2SiO_4), respectively. Furthermore, pH values of PBS consisting of nanofibrous composite scaffolds (Fig. 5(f)) increased from 7.4 due to the release of alkaline ions and then slightly decreased correlated to acidic products of PCL degradation. After surface modification and hydrolytic treatment, the significantly higher ($P < 0.05$) weight loss of scaffolds and more enhanced pH of PBS were obtained. It might be originated from leaching out of well distributed forsterite nanopowder through the scaffolds and hence increased porosity and permeability of the scaffolds.

3.2. Attachment and proliferation of MC3T3-E1 cells on nanofibrous PCL/forsterite scaffolds

In vitro cellular attachment was assessed by culturing MC-3T3 cells on the nanofibrous scaffolds cultured for 6 h. DNA quantification (PicoGreen assay) confirmed that forsterite nanopowder significantly enhanced the total DNA contents per unit-wet weights of the scaffolds compared to pure PCL ($P < 0.05$) (Fig. 6(a)). In addition to forsterite content, modification process dramatically modulated cell attachment. After surface modification, cell attachment on PCL/20 wt.% (M-Mg_2SiO_4) decreased compared to unmodified sample, while it was not significantly changed on PCL/5 wt.% (M-Mg_2SiO_4) scaffold. After hydrolytic treatment, cell attachment was significantly increased compared to other scaffolds. Hydrophilicity contributed to the physicochemical interaction between cells and biomaterials and the presence of hydrophobic dodecyl chains on the surface of forsterite particles resulted in decreased cell attachment compared to unmodified scaffolds [28–30]. After hydrolytic treatment, removing dodecyl chains and formation of Si – OH groups improved hydrophilicity resulted in significantly enhanced cell attachment. SEM image of MC3T3-E1 cells after 7 days of culture (Fig. 6(b)) showed the cells actively spread on the PCL/20 wt.%(MH(H)-Mg_2SiO_4) fibrous scaffolds with intimate adhesion to its porous surface. Due to the small pore sizes of the scaffold, cells remained on the surface and cannot penetrate in the depth of the structure.

The proliferation of MC3T3-E1 cells was also evaluated by AB assay (Fig. 7). AB assay revealed that the proliferation of cells significantly ($P < 0.05$) increased on various scaffolds with increasing culture time. Furthermore, cultured cells on composite nanofibrous scaffolds presented higher proliferation rates than those on pure PCL. Additionally, hydrolytic treatment resulted in significantly improved cell proliferation compared to unmodified scaffolds. It was about 145% and 161% within PCL/5 wt.% (MH(H)-Mg_2SiO_4) and PCL/20 wt.% (MH(H)-Mg_2SiO_4), respectively, compared to unmodified scaffolds after 7 days of culture. According to these results, in addition to the great ability of nanophase forsterite to support cell attachment and proliferation [3,9], the well-dispersion of Mg_2SiO_4 particles within PCL matrix and enhanced interaction between nanophase ceramics and cells could also enhance cellular proliferation. Furthermore, significant improvement of cell attachment and proliferation after hydrolytic treatment demonstrated the improvement of the hydrophilicity due to the removal of the alkyl chains.

4. Conclusion

In this study, forsterite (Mg_2SiO_4) nanoparticles, surface modified with dodecyl alcohol, were incorporated in PCL matrix in order to develop nanofibrous composite scaffolds. Then, surface modified forsterite nanopowder and the obtained nanofibrous composite scaffolds were treated in boiled water in order to remove the dodecyl chains. Through improved compatibility between filler and matrix, forsterite nanopowder could well disperse resulted in homogenous structure with smaller fibers as well as significantly enhanced mechanical properties. After hydrolytic treatment, the hydrophilicity of forsterite nanopowder and composite nanofibrous scaffolds was recovered resulted in improved degradation rate, bioactivity and cellular interactions. According to these data, surface modification of nanophase ceramic along with hydrolytic treatment of the scaffolds

was a feasible and effective method to fabricate composite nanofibrous scaffolds with significantly improved properties.

Acknowledgments

The authors are grateful for the support of this research by Isfahan University of Technology.

References

[1] M. Kharaziha, M.H. Fathi, Mechanically activated crystallization of phase pure nanocrystalline forsterite powders, Mater. Lett. 62 (27) (2008) 4306–4309.
[2] M. Kharaziha, M.H. Fathi, Synthesis and characterization of bioactive forsterite nanopowder, Ceram. Int. 35 (2009) 2449–2454.
[3] M. Kharaziha, M.H. Fathi, Improvement of mechanical properties and biocompatibility of forsterite bioceramic addressed to bone tissue engineering materials, J. Mech. Behav. Biomed. Mater. 3 (2010) 530–537.
[4] F. Causa, P.A. Netti, L. Ambrosio, A multi-functional scaffold for tissue regeneration: the need to engineer a tissue analogue, Biomaterials 28 (2007) 5093–5099.
[5] T.J. Webster, C. Ergun, R.H. Doremus, R.W. Siegel, R. Bizios, Specific proteins mediate enhanced osteoblast adhesion on nanophase ceramics, J. Biomed. Mater. Res. 21 (2000) 475–483.
[6] M. Diba, M.H. Fathi, M. Kharaziha, Novel forsterite/polycaprolactone nanocomposite scaffold for tissue engineering applications, Mater. Lett. 65 (2011) 1931–1934.
[7] M. Diba, M. Kharaziha, M.H. Fathi, M. Gholipourmalekabadi, A. Samadikuchaksaraei, Preparation and characterization of polycaprolactone/forsterite nanocomposite porous scaffolds designed for bone tissue regeneration, Compos. Sci. Technol. 72 (2012) 716–723.
[8] J. Venugopal, S. Low, A.T. Choon, A.B. Kumar, S. Ramakrishna, Electrospun-modified nanofibrous scaffolds for the mineralization of osteoblast cells, J. Biomed. Mater. Res. 85 (2008) 408–417.
[9] M. Kharaziha, M.H. Fathi, H. Edris, Development of novel aligned nanofibrous composite membranes for guided bone regeneration, J. Mech. Behav. Biomed. Mater. 24 (2013) 9–20.
[10] Z.K. Hong, P.B. Zhang, C.L. He, X.Y. Qiu, A.X. Liu, L. Chen, X.S. Chen, X.B. Jing, Nano-composite of poly(L-lactide) and surface grafted hydroxyapatite: mechanical properties and biocompatibility, Biomaterials 26 (2005) 6296.
[11] L. Borum-Nicholas, O.C. Wilson, Surface modification of hydroxyapatite. Part I. Dodecyl alcohol, Biomaterials 24 (2003) 3671.
[12] Q. Liu, J.R. de Wijn, C.A. van Blitterswijk, Nano-apatite/polymer composites: mechanical and physicochemical characteristics, Biomaterials 18 (1997) 1263–1270.
[13] S.C. Lee, H.W. Choi, H.J. Lee, K.J. Kim, J.H. Chang, S.Y. Kim, In situ synthesis of reactive hydroxyapatite nano-crystals for a novel approach of surface grafting polymerization, J. Mater. Chem. 17 (2007) 174–180.
[14] S.C. D'Andrea, A.Y. Fadeev, Covalent surface modification of calcium hydroxyapatite using n-alkyl- and n-fluoroalkyl-phosphonic acids, Langmuir 19 (2003) 7904–7910.
[15] H. Tanaka, M. Futaoka, R. Hino, K. Kandori, T. Ishikawa, Structure of synthetic calcium hydroxyapatite particles modified with pyrophosphoric acid, J. Colloid Interface Sci. 283 (2005) 609–612.
[16] H. Tanaka, M. Futaoka, R. Hino, Surface modification of calcium hydroxyapatite with pyrophosphoric acid, J. Colloid Interface Sci. 269 (2004) 358–363.
[17] L. Borum-Nicholas, O.C. Wilson, Surface modification of hydroxyapatite. Part II. Silica, Biomaterials 24 (2003) 3681–3688.
[18] D. Zhang, J. Chang, Effects of surface modification of β-$CaSiO_3$ on electrospun poly(butylene succinate)/β-$CaSiO_3$ composite fibers, Mater. Chem. Phys. 118 (2009) 379–384.
[19] Y.L. Zhou, Y. Gao, J. Chang, Effects of hydrolysis on dodecyl alcohol-modified bioactive glasses and PDLLA/modified bioactive glass composite films, J. Mater. Sci. 45 (2010) 6411–6416.
[20] M. Zhang, L. Ye, Y. Gao, X. Lv, J. Chang, Effects of hydrolysis on dodecyl alcohol modified β-$CaSiO_3$ particles and PDLLA/modified β-$CaSiO_3$ composite films, Compos. Sci. Technol. 69 (2009) 2547–2553.
[21] B. Wunderlich, Macromolecular Physics, vol. 3 Academic Press, New York, 1980.
[22] T. Kokubo, H. Takadama, How useful is SBF in predicting in vivo bone bioactivity? Biomaterials 27 (2006) 2907–2915.
[23] P. Weiss, M. Lapkowski, R.Z. Legeros, J.M. Bouler, A. Jean, G. Daculsi, Fourier transform infrared spectroscopy study of an organic mineral composite for bone and dental substitute materials, J. Mater. Sci.: Mater. Med. 8 (1999) 621.
[24] H. Tanaka, A. Yasukawa, K. Kandori, T. Ishikawa, Modification of calcium hydroxyapatite using alkyl phosphates, Langmuir 13 (1997) 821–826.
[25] J.G. Steele, C. McFarland, B.A. Dalton, G. Johnson, M.D.M. Evans, C.R. Howlett, P.A. Underwood, Attachment of human bone cells to tissue culture polystyrene and to unmodified polystyrene: the effect of surface chemistry upon initial cell attachment, J. Biomater. Sci. Polym. Ed. 5 (1993) 245–257.
[26] H.J. Lee, H.W. Choi, K.J. Kim, S.C. Lee, Modification of hydroxyapatite nanosurfaces for enhanced colloidal stability and improved interfacial adhesion in nanocomposites, Chem. Mater. 18 (2006) 5111–5118.
[27] Y. Gao, J. Chang, Surface modification of bioactive glasses and preparation of PDLLA/bioactive glass composite films, J. Biomater. Appl. 24 (2009) 119–138.
[28] J.H. Lee, S.J. Lee, G. Khang, H.B. Lee, Interaction of fibroblasts on polycarbonate membrane surfaces with different micropore sizes and hydrophilicity, J. Biomater. Sci. Polym. Ed. 10 (1999) 283–294.
[29] C.H. Kim, M.S. Khil, H.Y. Kim, H.U. Lee, K.Y. Jahng, An improved hydrophilicity via electrospinning for enhanced cell attachment and proliferation, J. Biomed. Mater. Res. Part B—Appl. Biomater. 78B (2006) 283–290.
[30] J. Wei, S.J. Heo, D.H. Kim, S.E. Kim, Y.T. Hyun, J.W. Shin, Comparison of physical, chemical and cellular responses to nano- and micro-sized calcium silicate/poly(epsilon-caprolactone) bioactive composites, J. R. Soc. Interface 5 (2008) 617–630.